Journal of *Marine Science and Engineering*

MDPI

Review

Climate Change and Tidal Hydrodynamics of Guadalquivir Estuary and Doñana Marshes: A Comprehensive Review

Inês Couto [1], Ana Picado [2], Marisela Des [3], Alejandro López-Ruiz [4], Manuel Díez-Minguito [5], Ricardo Díaz-Delgado [6], Rita Bastos [7] and João Miguel Dias [2,*]

1 Physics Department, University of Aveiro, 3810-193 Aveiro, Portugal; inesncouto@ua.pt
2 Centre for Environmental and Marine Studies (CESAM), Physics Department, University of Aveiro, 3810-193 Aveiro, Portugal; ana.picado@ua.pt
3 Environmental Physics Laboratory (EPhysLab), Centro de Investigación Mariña, Universidade de Vigo, Campus As Lagoas s/n, 32004 Ourense, Spain; mdes@uvigo.gal
4 Departamento de Ingeniería Aeroespacial y Mecánica de Fluidos, Universidad de Sevilla, Camino de los Descubrimientos s/n, 41092 Seville, Spain; alopez50@us.es
5 Andalusian Institute for Earth System Research, University of Granada, Avda. del Mediterráneo, s/n, 18006 Granada, Spain; mdiezm@ugr.es
6 LAST (Remote Sensing & GIS Lab) Doñana Biological Station-CSIC c/Américo Vespucio 26, Isla de la Cartuja, 41092 Sevilla, Spain; rdiaz@ebd.csic.es
7 Centro de Investigação em Biodiversidade e Recursos Genéticos (Centro de Investigação em Biodiversidade e Recursos Genéticos), Universidade do Porto, 4485-661 Vairão, Portugal; rita.bastos@gmail.com
* Correspondence: joao.dias@ua.pt

Abstract: The Doñana Protected Area, Western Europe's largest protected wetland and UNESCO World Heritage Site, is of great importance for the Spanish biodiversity. Despite its ecological value, there is a noticeable scarcity of scientific and technical information about its hydrology and expected climate change effects, as highlighted by several authors. This article reviews the existing research on the Guadalquivir River and Doñana National Park, examining the interplay between hydrodynamics, climate change scenarios, and the potential impact of the removal of the current dike which was built to limit tidal flooding. In this context, the hydrodynamic changes predicted by a hydrodynamic model were examined under both present (including the current mean sea level and the presence of the dike) and predicted future conditions (encompassing a mean sea level rise of 0.84 m and the removal of the dike). These hydrodynamic changes were assessed in terms of the maximum predicted water levels, mean velocity, amplitude, and phase of M_2 and M_4 tidal constituents, tidal asymmetry, and tidal prims. The results reveal that the removal of the dike and a sea level rise will have a significant impact on the protected area, resulting in the complete flooding of the Doñana national marshes during spring tides. Such changes could have negative impacts, as increased environmental alterations would require more demanding adaptation measures.

Keywords: Delft3D; climate change; maximum water levels; harmonic analysis; tidal prism

check for updates

Citation: Couto, I.; Picado, A.; Des, M.; López-Ruiz, A.; Díez-Minguito, M.; Díaz-Delgado, R.; Bastos, R.; Dias, J.M. Climate Change and Tidal Hydrodynamics of Guadalquivir Estuary and Doñana Marshes: A Comprehensive Review. *J. Mar. Sci. Eng.* **2024**, *12*, 1443. https://doi.org/10.3390/jmse12081443

Academic Editor: Dominic E. Reeve

Received: 16 July 2024
Revised: 14 August 2024
Accepted: 15 August 2024
Published: 21 August 2024

Copyright: © 2024 by the authors. Licensee MDPI, Basel, Switzerland. This article is an open access article distributed under the terms and conditions of the Creative Commons Attribution (CC BY) license (https://creativecommons.org/licenses/by/4.0/).

1. Introduction

Wetlands are amongst the most productive ecosystems globally, serving as diversity centres [1,2], playing a crucial role in supporting various species and maintaining ecological balance. Estuaries are intricate and dynamic systems, characterised by meaningful variability in physical and chemical gradients, making them among the most challenging aquatic environments [3,4]. Despite their high productivity as transitional coastal areas, they often face large disturbances. With over 60% of the global population residing in coastal areas [5], human activities have substantially altered estuarine ecosystems. Anthropogenic influences such as urbanisation, industrialisation, and agricultural practices have led to increased nutrient inputs, habitat degradation, and alterations in hydrological patterns within estuarine environments [3,6–10]. Moreover, the climate change-induced

sea level rise poses additional threats to these already vulnerable ecosystems. Beyond sea level rise, climate change is expected to induce a variety of complex physical processes.

Changes in the precipitation regime could alter freshwater inflow, affecting water discharge and sediment transport, leading to shifts in estuarine morphology and tidal dynamics.

Additionally, increased extreme weather events may cause more frequent flooding, altering salinity levels and impacting aquatic species. Rising temperatures could also affect biogeochemical processes, influencing nutrient cycling, water quality, and overall estuarine health.

The implications of such alterations extend beyond the immediate ecological realm, affecting the livelihoods of communities dependent on estuarine resources for sustenance and economic activities.

The Doñana Protected Area is the largest protected wetlands in Western Europe and a UNESCO World Heritage Site. The lowest part of the national park is parallel to the Guadalquivir Estuary and is isolated from estuarine tidal flow by a dike built in 1984 and floodgates.

Over the years, both the Doñana National Park and the Guadalquivir River have experienced substantial anthropogenic pressures. The Guadalquivir River holds a unique status as the only navigable river in Spain, providing access to Seville Harbour. The Doñana Marshes, on the other hand, contain a complex mosaic of natural wetland and artificial salt pans, rice fields, and fish farms within an inner delta [11]. Along with the increasing climate change events, such as droughts, rising temperatures and sea levels, these pressures further aggravate the challenges of preserving this delicate natural environment, impacting the habitats they offer and their capacity to regulate water quality and flooding [12]. Despite these ecosystems having great importance to Europe's biodiversity, the lack of information about them should be highlighted. In fact, several authors (Díez-Minguito et al., Spinosa et al., etc.) [13,14] have noted limited scientific research in certain fields and scarcity of available data on Guadalquivir Estuary. In a joint UNESCO/IUCN/Ramsar report, the mission team pointed out that the overall level of scientific uncertainty is unacceptable for an iconic World Heritage Site such as the Doñana National Park [15].

Nonetheless, two recent publications synthesise the available knowledge on the threats and status of Doñana's marshes and ponds, concluding that there is strong scientific evidence that groundwater abstraction has already caused major ecological damage to Doñana, and that this damage is increasing over time [16] and that Doñana wetlands are the most threatened ecosystem depicting a dramatic reduction in water amount, as a result of the intense and long drought events and uncontrolled water abstraction in the basin [17]. Some recent studies on the Guadalquivir Estuary, using numerical simulations, Sirviente et al. [18], have highlighted the significant impact of continuous dredging on the estuary's morphology. Changes in bottom depth, alongside alterations in channel width and depth, have been identified as critical factors influencing the resonant tidal response, specifically the M_2 tidal wave, and affecting tidal current intensity, particularly near the estuary's mouth. A 1D hydrodynamic model has shown that these morphological changes also play a crucial role in regulating trace gases within the estuarine ecosystem [18]. An analysis performed with a 3D numerical model (Delft3D-Flow) [19] further examined the nonlinear interaction of semidiurnal tidal constituents and tidal resonance, revealing that the estuary's tidal amplification factor varies with the spring-neap tidal cycle, with higher values during neap tides. This response is influenced by channel convergence, friction, and tidal reflection at the dam, with friction affecting both the amplification factor and wave speed of the tidal constituents, leading to greater amplification and speed for constituents of lower amplitude [19]. Additionally, a study using 'Satellite Radar Altimetry' [20] analysed the CryoSat-2 satellite's ability to measure sea level elevation caused by less-salty river discharge in coastal zones. From this study, it was found that freshwater bulges can increase sea levels by 5–10 cm up to 50 km from the estuary mouth [20].

While the full scope of climate change impacts on estuarine systems is vast and multifaceted, this study focusses specifically on the tidal hydrodynamic responses of the Guadalquivir River and Doñana Marshes to the projected sea level rise and the planned removal of a key dike infrastructure that completely isolates the marshes from the Guadalquivir River, Entremuros, and Brazo de la Torre tributary (Figure 1). These aspects have been identified as critical for understanding the future dynamics of this region, given its ecological significance and the direct influence of these factors on water levels, tidal regimes, and habitat conditions.

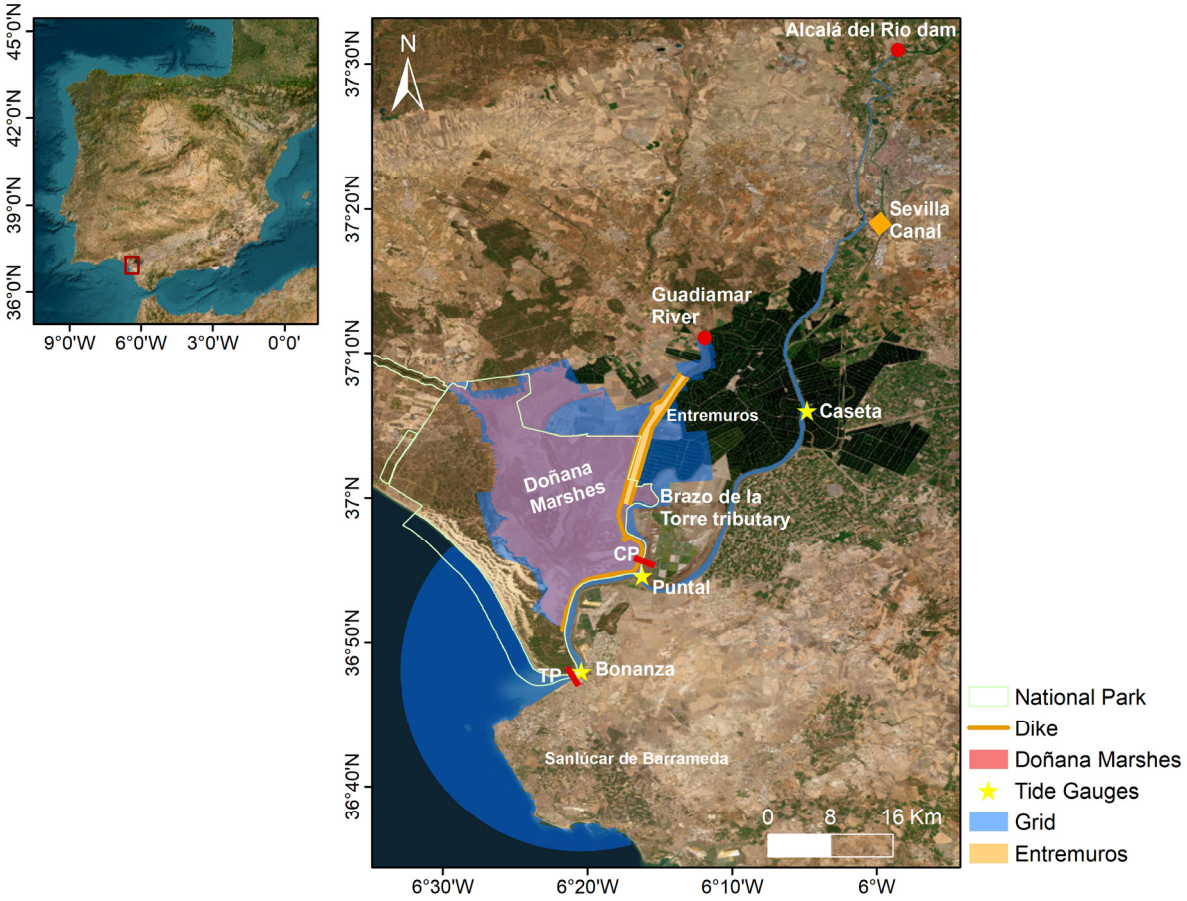

Figure 1. A map of the Doñana Marshes and Guadalquivir Estuary, with the national park delimited. The tide gauges (yellow stars) and cross-sections (red rectangles) where the tidal prism was computed are represented. The orange diamond marks the beginning of the Sevilla Canal that connects to the Guadalquivir River and the Port of Seville. The red circles identify the Guadiamar River and the Alcalá del Rio dam.

In this context, this article aims to deepen current research on the hydrodynamics of the Guadalquivir River and Doñana National Park, intending to contribute to overcoming the lack of information and knowledge about this system and to elucidate the consequences of both morphological changes, such as alterations in landscapes, and expected climate-induced changes. The goal is the characterisation of the Doñana Marshes and Guadalquivir Estuary under the current and future conditions, specifically focussing on the impacts of the projected sea level rise for the region and the potential morphological consequences of dike removal. By examining these factors, this study seeks to unravel the intricate interactions between human activities, natural processes, and environmental transformations in this ecologically significant and relevant protected area.

2. Study Area

2.1. Doñana National Park

The Doñana National Park (DNP) (Figure 1) includes the Doñana Natural Reserve, covering a total protected area of 53,835 ha. It holds the highest level of protection of the reserve being designated as a Ramsar site, an EU Special Protection Area, a biosphere reserve, and a UNESCO World Heritage Site [11,21].

It is located on the right bank of the Guadalquivir River Estuary (37°00′ N 06°36′ W), with an altitude ranging from sea level to 80 m [22]. It encompasses three different ecosystems: marshes, active sand dunes, and Mediterranean vegetation on top of the stabilised sand dunes [21,23]. In 1994, Siljeström et al. [24] studied the geomorphological characterisation of the DNP, through a soil–vegetation analysis, showing the details of the geographical evolution of the park during the Quaternary period and the climate change that occurred during that time. They revealed that the protected area had three primary morphogenetic systems (aeolian, estuarine, and coastal), with a Mediterranean climate and uneven rainfall distribution. It also emphasises the importance of understanding the park's Quaternary geographical history as a fundamental basis for understanding its current morphology and essential processes. To study the formation and evolution of the Guadalquivir Chenier plain in the Doñana Marshes, Rodríguez-Ramírez and Yáñez-Camacho [25], performed geomorphological and stratigraphic techniques, along with radiometrically dated cores to map spatial distribution. They showed that the Chenier formations constitute a Chenier plain containing transgressive ridges, regressive ridges, and laterally accreted ridges. These formations are crucial for the understanding of the paleoenvironmental aspects and future management of this coastline. As stated before, the Doñana region has a Mediterranean climate (dry subhumid) softened by oceanic influence. Precipitation is highly variable and unpredictable from year to year, with autumn typically being the rainiest period, having however, in some years, scarce precipitation that delays the main rains until winter or even spring [22,26,27].

2.2. Guadalquivir Estuary

The Guadalquivir Estuary, located on the Atlantic coast of southwest Spain, stretches 110 km inland from its mouth at Sanlúcar de Barrameda (Bonanza) to the Alcalá del Río dam (Figure 1). The current composition of the estuary includes a main shipping channel and a few tidal creeks, with no substantial intertidal zones present [13]. The width of the Guadalquivir River Estuary shows variations, ranging from 800 m near the mouth to 150 m at the uppermost part close to Seville Port. These variations follow a mild exponential decrease, and the convergence length, where the width tends to converge, is estimated to be approximately 60 km [13].

It holds the distinction of being the only navigable river in Spain, providing access to Seville Port. To ensure navigability, maintenance dredging is carried out periodically by Autoridad Portuaria de Sevilla (APS), to sustain a minimum navigation channel depth of 6.5 m, with the main channel depth averaging around 7 to 8 m [13,28].

The Alcalá del Rio dam (Figure 1) functions as a crucial control mechanism, managing the river's flow and acting as freshwater a barrier against incoming tidal waters [18]. When the tide reaches this dam, it possesses sufficient energy to reflect and interact with the incident wave. This interaction leads to tidal elevation exhibiting hypersynchronous patterns, forming a quasi-standing tidal wave pattern in the uppermost part of the river [29]. This was seen in a study conducted by Díez-Minguito et al. [29], in 2012, that investigated the turbidity and salinity dynamics in the Guadalquivir River Estuary, demonstrating that there are two estuarine turbidity maxima, one at 25 km from the mouth (near Puntal) and other near Port of Seville. In this stretch, the occurrence of a tidal wave reflection at the dam occurs, affecting tidal propagation and potentially influencing the spatial and temporal distribution of turbidity. Additionally, the study indicates that the sedimentation rate is increased, near the dam, by the most energetic tidal constituent, M_2.

The 1D numerical model used by Sirviente et al. [18] implemented realistic variations of breadth and bottom depth (averaged across the channel) that have been highly valuable for investigating amplification phenomena. This study, along with findings from Díez-Minguito et al. [29], confirms that the estuary shows a clear tendency to resonate, particularly enhanced by its deepening. This deepening reduces bottom friction and minimises the decrease in tidal wave amplitude as it travels through the estuary. The variations in depth, especially width, along the estuary are critical in determining the extent of the resonant response to the M_2 tidal wave.

The freshwater discharges from the dam exhibit a partial seasonality [30]. Over time, contributions of freshwater to the estuary have decreased, with an average reduction of about 60%. This reduction is more pronounced in dry-year cycles. During summertime, the flow is severely limited, while in late winter and early spring (the wet season), sporadic discharge occurs, typically following intensive rainfall episodes [13,31]. In a 11-year analysis (from 2012 to 2023) (Figure 2), 44% (1774 days) of the Guadalquivir River discharge is between 0 and 20 m^3/s, 40% (1598 days) ranges from 20 to 50 m^3/s, 14% ranges between 50 and 500 m^3/s, and the remaining 2% is above 500 m^3/s. During this period, the minimum discharge occurred on 3 November 2014, with a flow of 0.325 m^3/s, and the maximum discharge occurred on 13 March 2013, with a flow of 2032.9 m^3/s. The average river flow is 55.0 m^3/s.

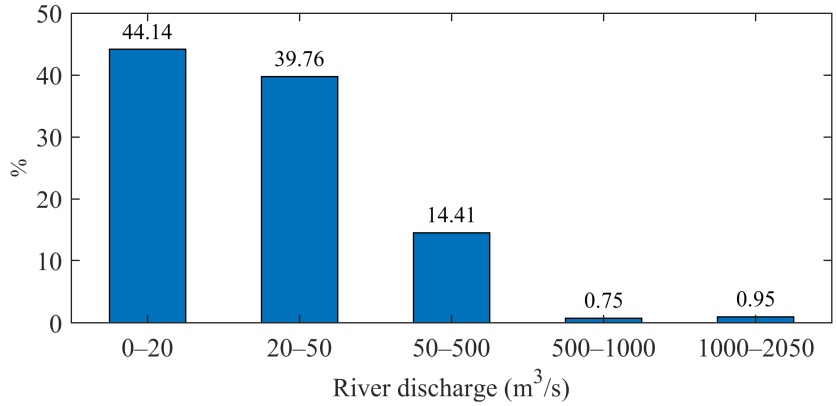

Figure 2. Guadalquivir discharge ranges in percentage (%) at the Alcalá del Rio dam for a 11-year period (2012 to 2023). Data were sourced from the website of the Confederación Hidrográfica del Guadalquivir (https://www.chguadalquivir.es/saih/DatosHistoricos.aspx, accessed on 1 October 2023).

An article published in 2014 by Díez-Minguito et al. [32] discussed the importance of turbidity in estuaries, which is measured by the absorption and scattering of light in the water due to the presence of dissolved organic matter and suspended particulate matter. The Guadalquivir Estuary is an example of an estuary with high concentrations of suspended sediments and frequent water quality problems. According to the authors, several extreme turbidity events occurred during extended periods with no freshwater discharge from the upstream dam, which have led to hypoxia downstream.

2.3. Doñana Marshes

The Doñana Marshes contain a complex mosaic of natural wetland and artificial salt pans, rice fields, and fish farms within an inner delta. To determine flooded areas in the Doñana Marshes, Díaz-Delgado et al. [33] used Landsat images to apply a semi-automatic procedure for the period 1973–2014. Recently the same author has updated this geospatial database up to 2022 [17]. Both studies confirmed that rainfall is the main driver of the flooding regime in the Doñana Marshes, and the time series analysis revealed two contrasting patterns in the hydroperiod of the Doñana Marshes: a substantial decrease in the southern area and an increase in the northwestern region. Under natural conditions, the

Doñana Marshes are flooded by direct rainfall, by the northern tributary streams and rivers, by the Brazo de la Torre shallow riverbed, and the tidal overflow from the Guadalquivir River. However, since 1998, the Doñana Marshes have been completely isolated from estuarine tidal flow and Brazo de la Torre by a remaining infrastructure (dike; see Figure 1). With rain being the main water input for the Doñana Marshes, Huertas et al. 2017 [34] evaluated the impact of the annual precipitation pattern on CO_2 exchange in the aquatic systems of Doñana and provided an initial analysis of the sink/source strength of the wetlands under contrasting hydrological cycles. It showed that during extremely wet cycles, flooded systems exhibit the highest CO_2 emissions, while under drier conditions, CO_2 fluxes diminish, and some areas even act as mild sinks for atmospheric CO_2. The study showed that the ecosystem of the Doñana wetlands acts as a large CO_2 sink, with regional air–water carbon transport varying based on meteorological conditions. Later on, Huertas et al. 2019 [35] assessed the spatio-temporal variability of methane emissions from the salt marshes of the Doñana Wetlands in Spain, identifying the controlling factors and providing a baseline for future studies on the impact of climate change and human management interventions. The strong correlation between methane and temperature suggests that temperature significantly regulates methane production in these wetlands, concluding that the Doñana salt marshes emit methane moderately. Temperature, phytoplankton activity, and salinity are identified as the primary drivers of methane formation. The study also emphasised the need to explore the potential impact of lateral tidal pumping, methane ebullition fluxes, and plant-mediated methane transport in future research.

2.4. Aznalcollar Mining Spill (1998)

On 25 April 1998, a mining spill accident occurred in the Aznalcollar mine that lasted 5 days. It spread approximately 4 million m^2 of acidic water and 2 million m^2 of toxic mud containing high amounts of heavy metals. Approximately 4 Hm^3 of the polluted mud and water were directly discharged into the Guadalquivir River [21,36,37]. The areas within the protected area overflowed by the mine tailing wastes were 2656 and 98 ha, respectively, representing 4.2 and 0.19% of the total park surface, respectively [21]. The toxic waters were retained by several dikes and dams constructed urgently in the Entremuros area (Figure 1), one of the main inundation drivers, reducing marsh tidal flooding [21,36,38]. To isolate the marshes from the toxic waste discharge arriving via Guadiamar river (Figure 1), authorities performed as an urgent action the building of an additional dike that completely isolated the marshes from the Guadalquivir River, Entremuros, and Brazo de la Torre [23]. Since then, the permeability control of the dike is achieved through floodgates distributed throughout the infrastructure [23].

Studies from Grimalt et al. [21] and García-Luque et al. [36] both provide a deep description of the effects of the Aznalcollar spill. In 1999, Grimalt et al. [21] introduced the environmental consequences of the Aznalcollar mine accident in Spain, focussing on Doñana Park, and later, in 2003, García-Luque et al. [36] showcased the importance of studying heavy metal concentrations in the Guadalquivir Estuary after the mining spill. Grimalt et al. [21] outlined the mining activities and immediate mitigation efforts and emphasised the ongoing studies investigating the accident's long-term effects. Their objective is to provide readers with an understanding of the detailed studies featured in the article, placing them in the wider context of environmental challenges resulting from the accident. As for García-Luque et al. [36], their work presents and underscores results that exhibited high concentrations of inorganic carbon and the high residence time of sulphate.

In 2005, an ambitious restoration project for Doñana Marshes, named 'Doñana 2005', was conducted with the main goal of recovering the quantity and quality of tributary water in the freshwater marsh [23,38]. One of the planned actions was to remove the dike in the future to re-establish the connection between the Doñana Marshes and Guadalquivir River through its arm, Brazo de la Torre [23].

3. Data and Methods

3.1. Hydrodynamic Model

The Delft3D model suite is a very accurate tool for simulating the Guadalquivir Estuary's hydrodynamics. It solves the 3D baroclinic Navier–Stokes and transport equations under the Boussinesq assumption [39].

In a previous investigation, Wang et al. [40] used Delft3D to study sediment transport in the Guadalquivir Estuary during dry periods. They noticed that when suspended sediment concentrations were high, a net transport of sediments out of the estuary occurs due to its proximity to the deep Atlantic Ocean with low sediment concentrations. The field data on suspended sediment concentration support the idea that variation in concentration explains hydraulic resistance.

In this work, an implementation of Delft3D in the Guadalquivir Estuary was addressed. It considered a curvilinear grid with 872 × 2400 cells, with higher resolution in the area closer to the Guadalquivir River (68 × 16 m) and the tributary (Brazo de la Torre) (42 × 17 m) (Figure 1).

Bathymetric data were provided under the scope of the PIRATES project (Multi-criteria analysis for Physical and bIotic Risk Assessment in EStuaries) and of the EU Horizon 2020 project eLTER PLUS European Long-Term Ecosystem. Moreover, critical zones and socio-ecological systems infrastructure research were obtained from PLUS' (grant agreement no. 871128) under task 8.1, 'High resolution biodiversity data to assess environmental change', in collaboration with the Doñana Biological Station. The topographic data for the Doñana Marshes were obtained by using the Digital Elevation Model (DEM) produced from a LiDAR flight carried out in September 2002, by the companies GEA CARTOGRAFÍA and FOTONOR, with a 2 m horizontal spatial resolution and a nominal vertical resolution of 0.15 m (ref) [41].

The primary driving force governing the circulation within the estuary is the propagation of tides; so, at the oceanic boundary, the amplitude and phase of the local tidal constituents were implemented, obtained from the OSU TOPEX/Poseidon 8.0 model Global Inverse Solution (https://sealevel.jpl.nasa.gov/missions/topex-poseidon, accessed on 1 October 2013). A single freshwater source was introduced as the fluvial boundary, reflecting the main source of freshwater input to the Guadalquivir Estuary originating from the Alcalá del Rio Dam. The circulating river flow data, in m^3/s, from the Alcalá Dam, were employed, sourced from the Confederation Hidrográfica del Guadalquivir website (https://www.chguadalquivir.es/saih/DatosHistoricos.aspx, accessed on 1 October 2013).

Additionally, the dike infrastructure was established with a 3 m height on average (Figure 1), implemented as a 2D weir (.2DW) function. The roughness input was defined as a water-depth-dependent roughness formulation offered by the trachytopes function.

The model used for this study was based on a grid developed in a previous implementation that only considered the Guadalquivir Estuary and was validated with current and sea level data from [42]. Additionally, the Doñana Marshes and the dike were included in the grid, and the validation of the numerical model for the Guadalquivir Estuary and Doñana Marshes was performed by Couto [43], through the comparison between the model's results and observed data of water levels and amplitude and phase of the main tidal constituents (M_2, S_2, O_1, K_1, and N_2) at three stations (Bonanza, Puntal, and Caseta; see Figure 1). The results indicate that the model accurately reproduces the tide, with root mean square errors between 9 and 18 cm, with an error range of 4–8%. The largest error is observed at the upstream station, Caseta, while the best agreement was achieved at the station nearest to the estuary mouth, Bonanza. The results are illustrated in Figure S1.

3.2. Simulation Design

The global mean sea level has risen approximately 21 cm since 1900, and projections suggest a continued rise by 2100 [44,45]. This increased trend is anticipated to have pronounced impacts, particularly in coastal areas characterised by high exposure and vulnerability [46].

According to the projections from the 6th Assessment Report (AR6) by the Intergovernmental Panel on Climate Change (IPCC) [47] for a long-term period (2081–2100) relative to the baseline period of 1995–2014, a sea level rise of 0.84 m is expected in the Guadalquivir Estuary region for Scenario SSP5-8.5. This scenario is the most pessimistic and illustrates very high greenhouse gas emissions and CO_2 annual emissions tripling by 2080. The projection was derived using the Sea Level Projection Tool provided by NASA [48].

Additionally, morphological changes can also significantly impact the delicate balance of coastal environments, such as the Guadalquivir Estuary and Doñana Park. These changes can disrupt established hydrodynamic patterns, influence sediment dynamics [49], and, consequently, have far-reaching effects on the biodiversity, habitat suitability, and overall ecological resilience of these vital coastal zones.

In this context, it is crucial to characterise the study area under current conditions and juxtapose it with anticipated future conditions, considering the projected sea level rise for the region and the planned removal of the dike. The intentional aspect of removing the dike lies in establishing a connection between the salt marsh and tidal influences [23], and the marshes act as sinks for CO_2 and CH_4 [35]. Therefore, the present hydrodynamic situation was characterised, and comparisons between present and future conditions were performed, regarding maximum predicted water levels, amplitude and phase of the main harmonic constituents, average velocity (V_{RMS}), tidal prim, and tidal asymmetry. The present conditions account for the dike infrastructure and the present mean sea level, while future conditions account for the removal of the dike and a sea level rise of 0.84 m.

4. Hydrodynamic Characterisation of the Guadalquivir Estuary and Doñana Marshes

In this section, the hydrodynamic characterisation of the Guadalquivir Estuary and Doñana Marshes is discussed, with a specific focus on understanding the potential impact of the removal of the dike infrastructure on the Doñana Marshes, under both present conditions and expected climate change conditions.

4.1. Maximum Predicted Water Levels

The Guadalquivir River is characterised as a well-mixed estuary, inhibiting very small vertical salinity/temperature gradients. It is classified as a mesotidal estuary, primarily experiencing a semidiurnal period. The main driving mechanism is the tidal forcing at the mouth, resulting in a tidal range of 3 m [13,32].

The maximum predicted water level (mPwL) for the Guadalquivir Estuary is represented in Figures 3 and 4, for both present and future conditions, respectively, during spring and neap tides. For spring tide, the MPWL corresponds to the highest water level recorded. For neap tide, it corresponds to the lowest peak from the maximum water level recordings.

In spring tide (Figure 3a), the maximum water level in the estuary varies from 1.8 m at the mouth decreasing upstream to 1.3 m at the dam. Through the middle of the channel, the MPWL is uniform. Beyond Caseta, up to the Sevilla Canal, there is an increase to approximately 1.6 m, nearly matching the value at the inlet. During the neap tide (Figure 3b), a similar pattern persists: the highest values are found around the estuary mouth, gradually decreasing further up the river, with an increase in the levels in the Caseta–Sevilla stretch also. Interestingly, the area near the Sevilla Canal presents a larger maximum level compared to the area near Bonanza (e.g., near the ocean entrance, it is approximately 0.37 to 0.40 m, and near the Sevilla Canal, it is 0.45 m).

Upon analysing both spring and neap tide maps in the maximum predicted water level, it is evident that the maximum water levels decrease upstream until the middle of the estuary, and from there, it shows an increase, with the higher level both in the estuary mouth and in the area between Caseta and Sevilla Canal. The spring tide results are more than twice as high as the neap tide results.

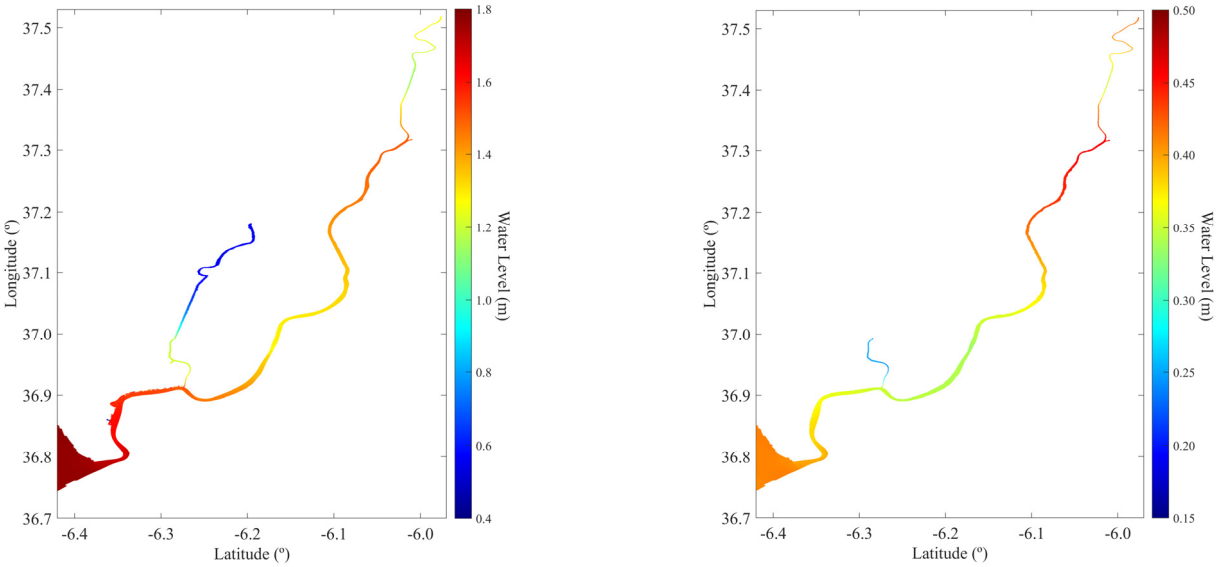

Figure 3. Maximum predicted water levels (MPWL) for (**a**) spring and (**b**) neap tides, for present conditions.

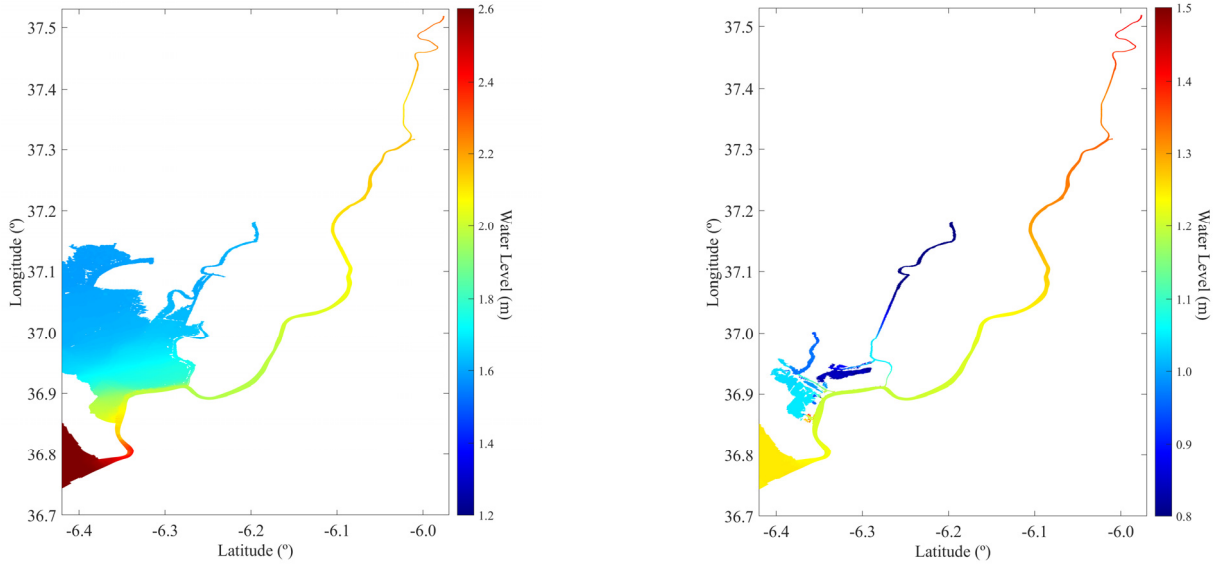

Figure 4. Maximum predicted water levels for (**a**) spring and (**b**) neap tides, for future conditions.

For future conditions during spring tide (Figure 4a), the MPWL follows an opposite pattern in the main channel when compared to the present (Figure 3a), as there is a general increase in the maximum levels upstream. This pattern is generally observed in neap tide under present conditions. During spring tide, for future conditions, the first stretch of the river near the beginning of the marshes experiences maximum levels ranging from 2.4 m to 2.2 m. After that region, the level gradually increases from 2.0 m to 2.3 m at the dam, recovering almost the same level as the inlet. For this scenario, due to the absence of the dike and a rise in the sea level, the seawater spreads over almost the entire study area. The maximum water level near the river borders is around 2 m, gradually decreasing to 1.7 m moving up the Doñana Marshes. During neap tide (Figure 4b), the same increasing pattern as spring tide persists. The main difference is observed in the inlet where it presents a more subtle maximum level. Also in the neap tide, there is water in the lower area of

Doñana Marshes, near the branches. If the decision would be to completely remove the dike infrastructure, adopting a gradual approach could be the optimal strategy for restoring the Doñana Marshes to its "original" state. As illustrated water spreads across the entire area in a climate change scenario, and the overall flow could lead to more drastic changes in the Doñana protected marshland, taking a step back in restoring it to the "original" state.

Considering a situation where only the dike is removed while maintaining the current sea level, the MPWLs are similar to those observed in Scenario 1 for both neap and spring tides. However, during spring tide, there is a noticeable inflow of water from the lower branches of the Guadalquivir Estuary into the Doñana Marshes. Furthermore, when considering a situation with a 0.84 m sea level rise while maintaining the dike, model results indicate that during spring tide, water extends beyond the location of the original dike, particularly in the tributary areas, though it does not penetrate much further inland. From a water level perspective, this suggests that the existing infrastructure could potentially contain almost all the inflow from both the sea and the river into the Doñana National Park, even under conditions of significant sea level rise.

According to Donázar-Aramendía et al. and Ruiz et al. [10,28] the Guadalquivir River Estuary faces various pressures, including regular dredging, unnatural freshwater inputs in summer for rice agriculture, permanent turbidity, and high regulation of the natural flow by the upstream dam, all of which hinder the development of diverse communities in the main channel. The connection between Doñana Marshes and the inlet could lead to better growth in diversity. However, the intrusion of saline water can alter the aquatic plant communities and potentially enable the spread of alien species. And also, as mentioned by Huertas et al. [34], connecting the Guadalquivir Estuary and Doñana Marshes may lead to a reduction in aquatic CO_2 emissions from the marshes. This is primarily due to the efficient removal of large volumes of suspended and organic material during wet years and the prevention of desiccation during prolonged droughts.

4.2. Root-Mean-Squared Velocity

The root-mean-squared velocity (V_{RMS}) provides a measure of the current intensity or energy associated with water movement at specific locations. Higher V_{RMS} values indicate a more energetic or turbulent water condition. Lower values suggest calmer or less turbulent conditions.

For present conditions, during spring tide (Figure 5a), higher velocity is observed near the Bonanza station at the estuary mouth, with a V_{RMS} ranging from 1.0 to 1.2 m/s. Towards the upstream, these values decrease to approximately 0.2 m/s near the dam. Between the Sevilla Canal and near the dam, where the Guadalquivir channel becomes shallower and narrower, the V_{RMS} increases, reaching 0.5 m/s, because the same volume of water flows through a smaller area, causing the velocity to rise. Through neap tide (Figure 5b), the pattern remains consistent, with higher V_{RMS} values observed in the lower section of the river, decreasing towards the head of the estuary. When comparing both spring and neap tides, it becomes evident that, during spring tides, the V_{RMS} is roughly twice as high as in neap tides for the whole Guadalquivir area. This difference is more pronounced in the lower and central estuary.

In the context of future conditions, during spring tide, an identical pattern of V_{RMS} is predicted throughout the main channel, nevertheless, with higher velocities. As water enters the national park, the velocities range from 0.3 m/s to around 0.6 m/s, decreasing upstream. During neap tide (Figure 6b), the pattern and variations for future conditions are similar to present conditions, with a decrease in velocity from the mouth to the dam. Also, the V_{RMS} is approximately half of the spring tide velocity. Considering the situation without the dike, the V_{RMS} pattern and magnitude are quite similar to the reference scenario, while for the situation in which the dike is maintained and the sea level is raised, the V_{RMS} is slightly higher than in Scenario1.

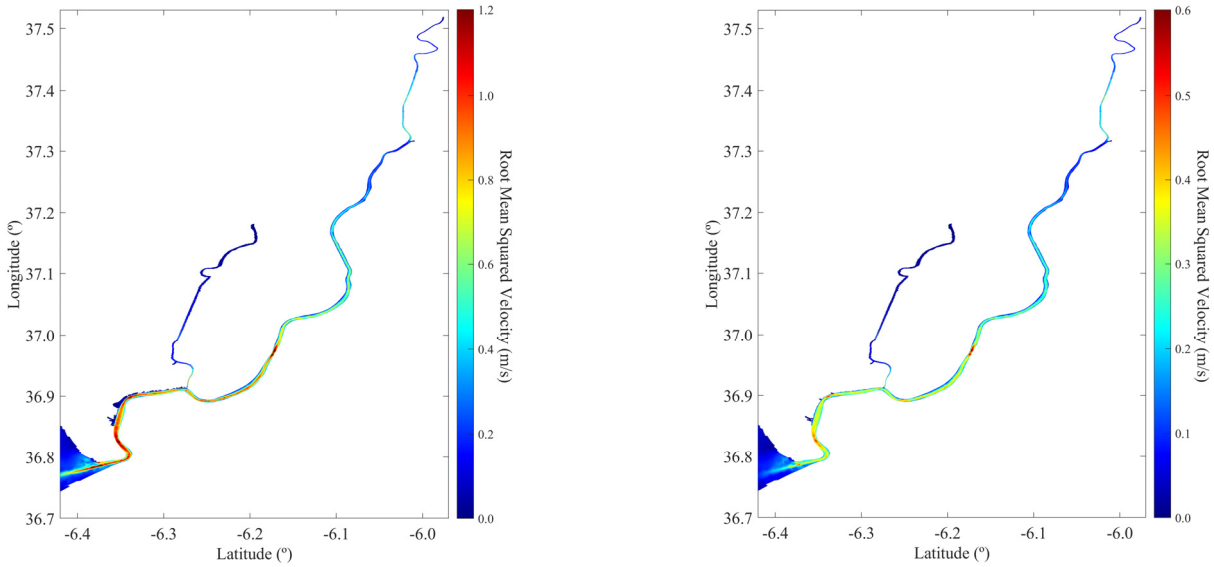

Figure 5. Average current velocity (V_{RMS}) at (**a**) spring and (**b**) neap tides, for present conditions.

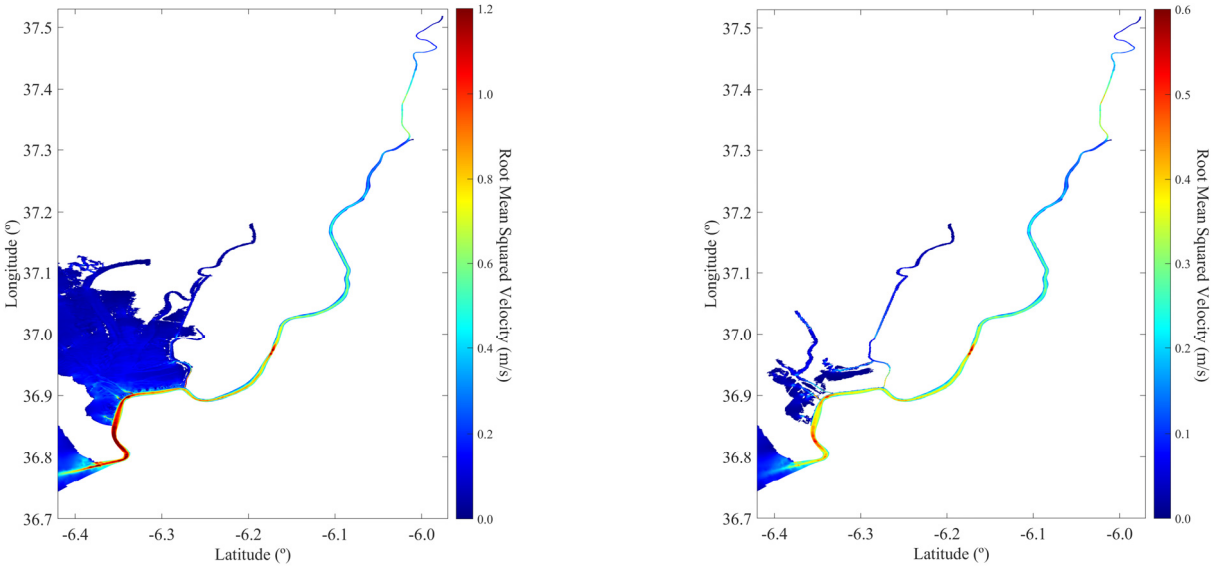

Figure 6. Average current velocity (V_{RMS}) at (**a**) spring and (**b**) neap tides, for future conditions.

4.3. Harmonic Analysis

The amplitude of the M_2 constituent at the mouth is approximately 1 m, with additional contributions from other relevant semidiurnal and diurnal constituents [13,31]. Some studies used the harmonic constituents to analyse the estuarine dynamics; in particular, García-Lafuente et al. [31] focussed on the Guadalquivir Estuary's tidal oscillations of water temperature, more specifically on sea surface temperatures in the Gulf of Cadiz. Examining an 18-month time series, the research utilised harmonic analysis to investigate tidal frequency signals. The results showed a notable dependence of harmonic analysis on the seasonal cycle of the collected data.

Short-term analyses centred on April and October exhibit minimal amplitude in the local water temperature signal for semidiurnal constituents, whereas longer series reveal a small M_2 amplitude. The study underscores the prominence of the S_1 constituent (radiational origin), nearly twice the gravitational counterparts (S_2 and M_2).

The amplitude and phase of the M_2 and M_4 tidal constituents [50] are represented in Figures 7–10 for both present and future conditions. This analysis allows the quantification of the specific tidal component's contribution to the overall tidal signal at a particular location (strength or magnitude) by the amplitude and the timing or position of the harmonic constituent by the phase of the tidal constituents. The harmonic analysis was computed on cells that were submerged for at least 55% of the simulation time.

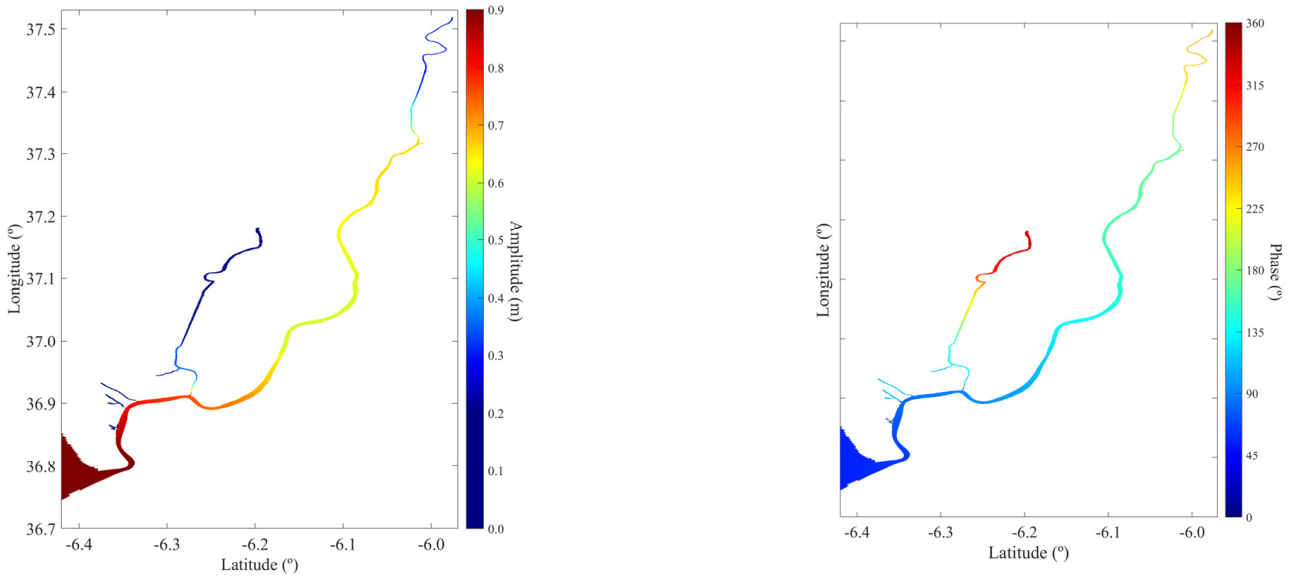

Figure 7. (**a**) Amplitude (m) and (**b**) phase (°) of the constituent M_2 for the study area for present conditions.

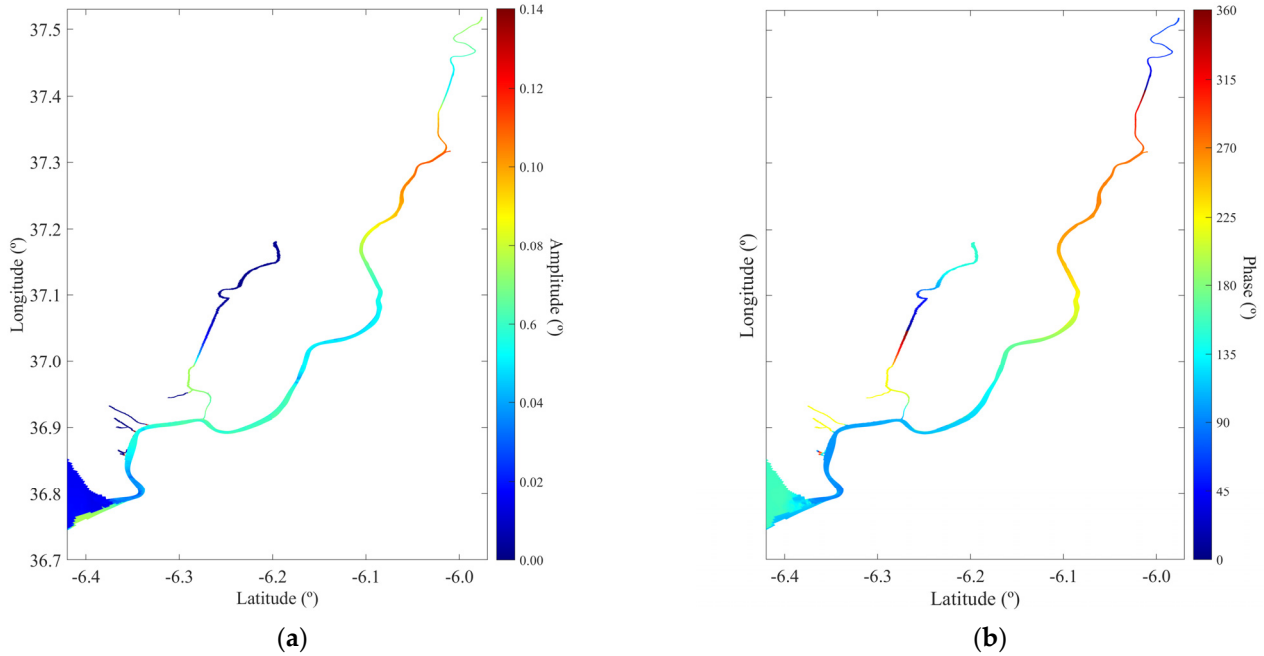

Figure 8. (**a**) Amplitude (m) and (**b**) phase (°) of the constituent M_4 for the study area for present conditions.

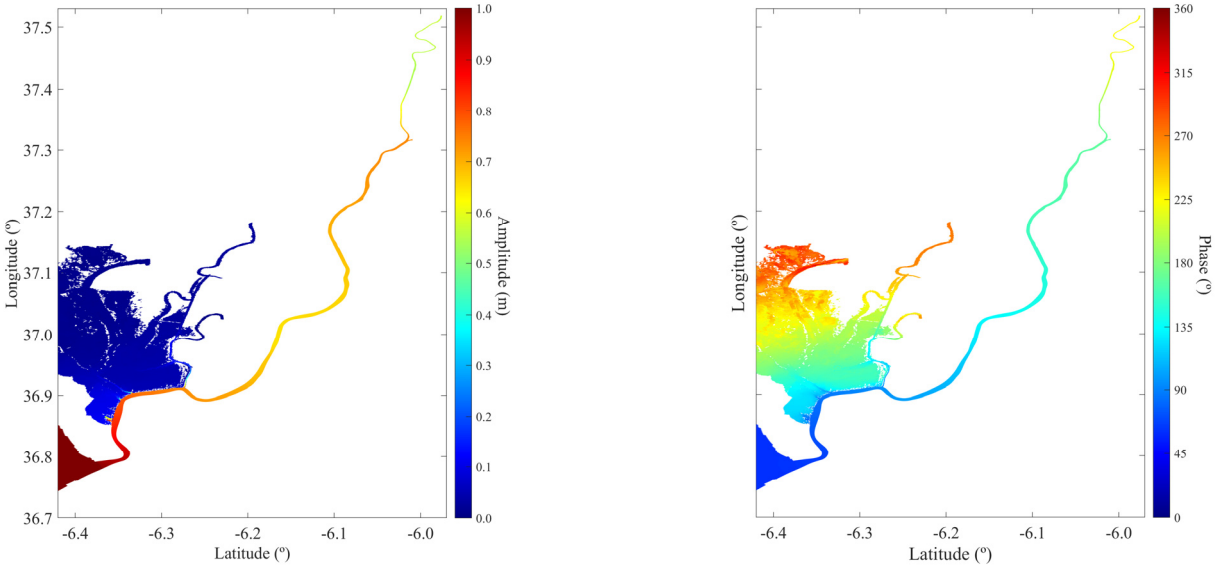

Figure 9. (**a**) Amplitude (m) and (**b**) phase (°) of the constituent M_2 for the study area for future scenario.

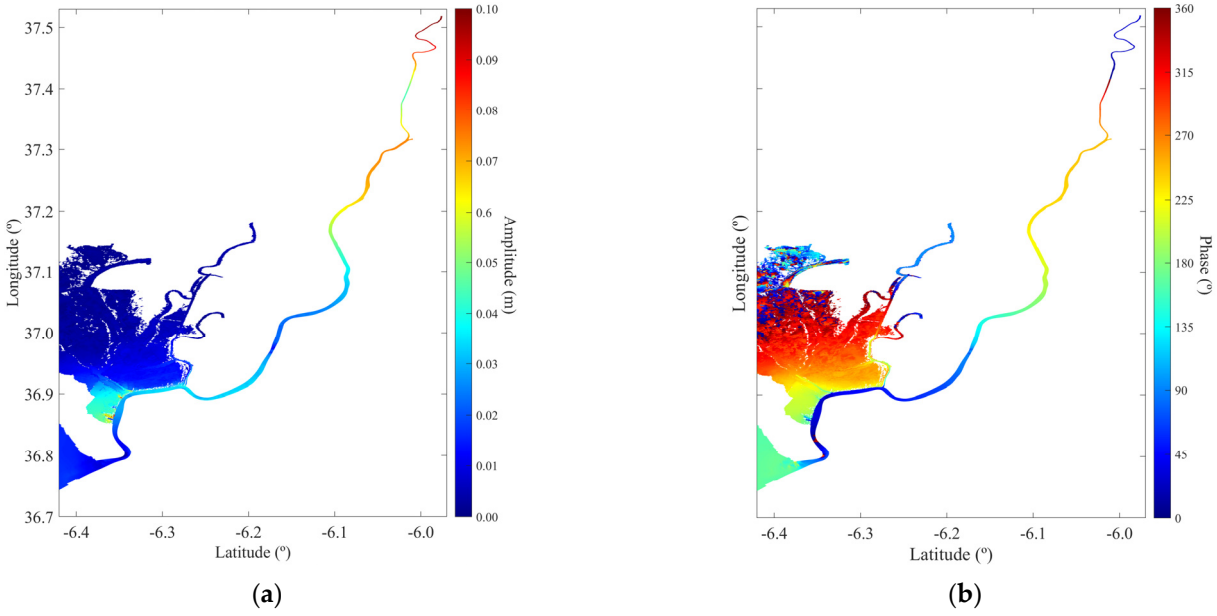

Figure 10. (**a**) Amplitude (m) and (**b**) phase (°) of the constituent M_4 for the study area for the future scenario.

When analysing Figure 7, which depicts the amplitude (m) and phase (°) of the M_2 constituent, it becomes evident that the amplitude (Figure 7a) decreases gradually along with an increase in phase from the inlet to the estuary head. This results in a difference of nearly 0.6 m from the estuary's mouth to the dam. The amplitude of the M_2 constituent decreases by approximately 50% from the river's mouth to the uppermost part of the dam. This pattern is also observed from the river mouth to the end of the tributary (Brazo de la Torre). Concerning the phase of the M_2 constituent (Figure 7b), it varies from 80° to 90° at the mouth of the estuary to 250° at the estuary head, resulting in approximately 6 h difference. In Brazo de la Torre, the phase increases in a shorter distance from 130° to 360° (8 h difference). The analysis confirms that the principal semidiurnal constituent, M_2, holds the greatest influence.

Regarding the M_4 constituent, Figure 8 represents the amplitude (Figure 8a) and phase (Figure 8b) distribution throughout the estuary, for the present conditions.

The results show that the amplitude of this constituent increases from around 0.02 m at the Bonanza Station to 0.06 m at the lower centre of the channel. It then decreases near the Caseta Station, followed by an increase to 0.10 m near the Sevilla Canal. Thereafter, it gradually decreases from 0.10 m to 0.06 m close to the dam. In general, the amplitude of M_4 increases from the inlet to the head of the estuary. Concerning the phase of the M_4 constituent, it starts at 100°, increases to 360°, and then begins the cycle again from 0° to approximately 50°. So, in terms of phase, the M_4 constituent exhibits an overall increase from the estuary's mouth to the head. From this analysis, it becomes more evident that, overall, tidal amplitudes decrease gradually from the estuary mouth to the dam's end channel. This is accompanied by a growth in the phase lag, showing that the tides are influenced by changes in a channel's topography.

Regarding the amplitude and phase of the harmonic constituents, considering a sea level rise and the dike removal (future conditions), the semidiurnal, M_2, is still the harmonic constituent that has the greatest influence. An increase between 0.1 and 0.2 m in its amplitude is predicted for the future (Figure 9a). For instance, at Caseta Station, the M_2 amplitude increases from around 0.55 m under the present conditions to 0.7 m under future conditions. At Doñana National Park, the amplitudes of M_2 are almost the same for the entire area (around 0.1/0.2). Regarding the M_2 phase (Figure 9b), there is a smaller increase from the inlet to the dam, approximately 15°, when compared to the present. In the future scenario, the phase behaves like a progressive wave, with the phase increasing upstream in the Doñana Marshes and in the tributary. Considering only the removal of the dike, both the amplitude and phase of M_2 are quite similar to the results found for Scenario 1. However, when the sea level rise is considered, an increase in M_2 amplitude is predicted, while the phase remains similar to Scenario 1.

Concerning the M_4 amplitude constituent in the future scenario (Figure 10a), a similar pattern to that observed in the present conditions is evident, however, with an increase of around 0.05 m between Caseta station and Sevilla Canal (0.07 m). In the Doñana National Park, in general, the amplitude decreases upwards, from around 0.05 m to almost 0 m.

Regarding the phase (Figure 10b), in the main channel of the Guadalquivir Estuary, it increases upstream, following a similar pattern to the current scenario. The main difference is in the lowest part near Doñana, where the phase is lower, around 45°, compared to about 120° in the present scenario (difference of 1.3 h). For Doñana National Park, just like for M_2, it increases the phase upwards; however, the phase of M_4 near the river starts at a higher value, starting a new cycle from the upper-central part of the park. Regarding the separate effects of dike removal and sea level rise, no significant changes in the M_4 amplitude and phase are observed, except near the dam, where the amplitude is higher in the sea level rise scenario compared to the reference.

4.4. Tidal Asymmetry

The Guadalquivir Estuary is dominated by tidal forcing, making it a flood-dominant environment, as mentioned in the study of Díez-Minguito et al. [13,43]. In 2012, Díez-Minguito et al. [13] studied tidal dynamics in the Guadalquivir Estuary, focussing on tidal propagation under varying river flows. The estuary was found to be predominantly tidally dominated for most of the year, with three distinct sections influenced by different tidal processes. When river discharge exceeded 400 m^3/s, the estuary shifted to a fluvially dominated state, displaying intermediate fluvial–tidal regimes. Tidal reflection at the dam was identified as a factor generating residual currents, impacting bed morphology. Specifically, the M_4 constituent favoured sedimentation near the dam, while the M_2 reflection extended potential sedimentation near the entrance of the Port of Seville, a crucial area for dredging operations.

As previously referred, an increase in the amplitude of the M_4 from the estuary's mouth to upstream is evident, which could lead to fluctuation in the duration of the

flood and ebb flows, indicating an asymmetrical tide. The tidal asymmetry magnitude is quantified through the amplitude ratio (Ar) and the orientation by the relative phase (φ). The amplitude ratio is determined using the amplitudes of the M_4 and M_2 constituents through the following equation:

$$Ar = \frac{A_{M_4}}{A_{M_2}}, \quad (1)$$

and the relative phase is determined through their phase,

$$\varphi = 2\theta_{M_2} - \theta_{M_4}. \quad (2)$$

In terms of the amplitude ratio (ar) (Figure 11a), near the mouth of the estuary, the ratio is approximately 0.02 m, gradually increasing to around 0.20 m as one moves closer to the dam. A similar pattern is observed in the tributary, indicating that the ratio increases with the distance from the estuary's inlet and suggesting that the tides become more asymmetric upstream, while still having a smaller value through the channel.

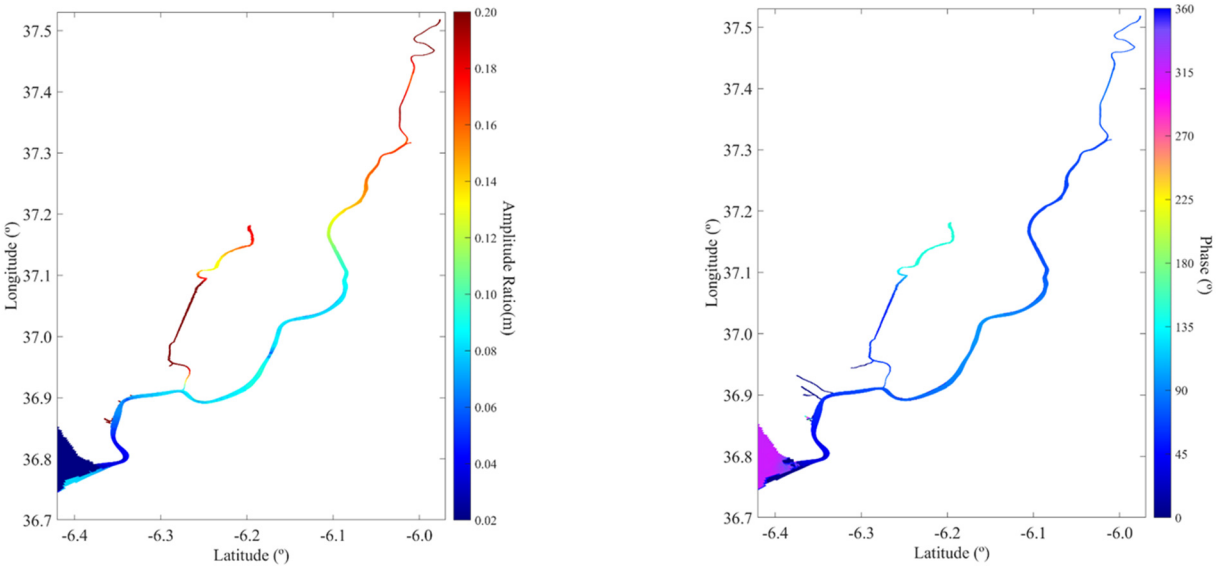

Figure 11. (**a**) Amplitude ratio (m) and (**b**) relative phase (°) for the study area for the present conditions.

The analysis of the relative phase (φ) (Figure 11b) indicates that the entire estuary experiences a flood-dominant pattern, as the phase throughout the area generally remains below 150°.

Regarding the future scenario (Figure 12a), the main channel presents a smaller asymmetry in tidal amplitudes for a larger extension than in the present conditions. In the Doñana National Park, the amplitude ratio presents a relatively larger asymmetry compared to the main channel, which leads to a higher dominance of the ebb or flood cycle. The relative phase (Figure 12b) for the future conditions has an overall phase below 180°, indicating that the Guadalquivir Estuary remained flood-dominant, taking more time to reach low tide than high tide. The Doñana Park, in general, is also flood-dominant. Considering the single effect of the dike removal and of the sea level rise, no significant changes were predicted when only the dike was removed. However, under sea level rise, the amplitude ratio and relative phase decreased compared to the reference scenario, indicating that the tide becomes less asymmetric while remaining flood dominant.

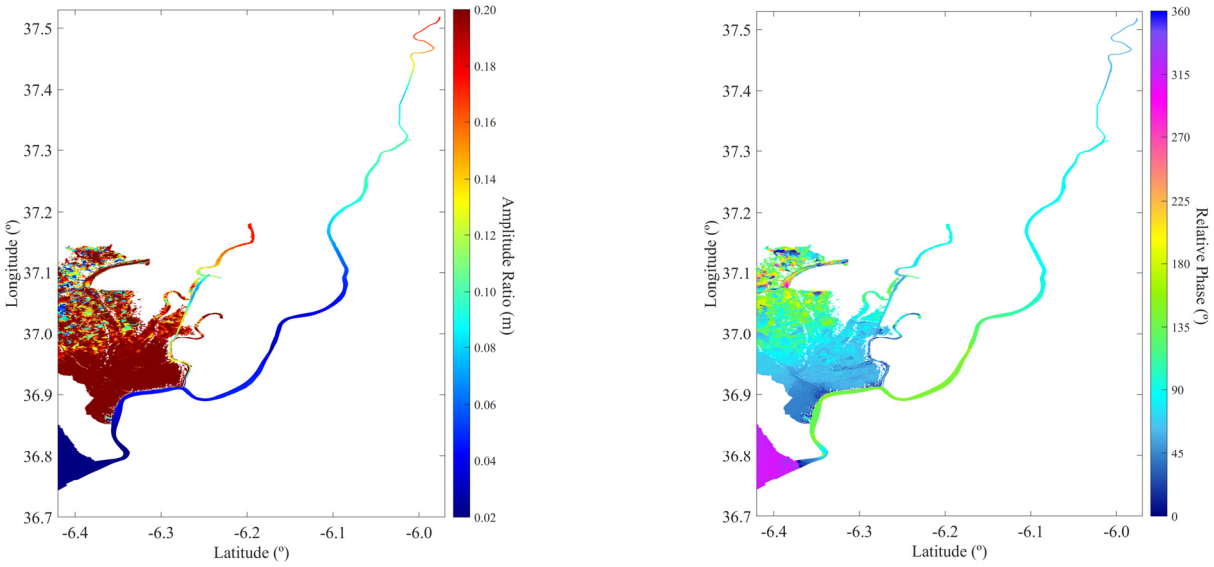

Figure 12. (**a**) Amplitude ratio (m) and (**b**) relative phase (°) for the study area for the future scenario.

4.5. Tidal Prism

The tidal prism, which is the volumetric flow that crosses a section in a flood cycle, depending on the location of the section and the tidal amplitude, was evaluated at the Guadalquivir inlet (TP in Figure 1) and the tributary Brazo de la Torre (CP in Figure 1), during spring and neap tide. Additionally, the volumetric flow was also evaluated for the ebb cycle, being called in this study tidal prism during the ebb cycle.

For the inlet cross-section TP (Figure 13a) and CP (Figure 13b), it is evident that the volume of seawater entering the estuary during flood cycle is greater than the volume of water leaving during ebb cycle for both spring and neap tide conditions. Additionally, during spring tide, the volume of seawater is also larger than during neap tide, as expected. Considering the single effect of the dike removal and of the sea level rise, an increase in the tidal prism is predicted for both sections compared to present conditions. Moreover, in the future scenario that evaluates the combined effect of dike removal and sea level rise, the tidal prism further increases. This is justified by the higher tidal amplitude for future conditions, as a direct consequence of rising sea levels.

For the first cross-section (TP), which is closer to the Bonanza Station and the inlet, the volume of water that flows during flood and ebb cycles in neap tide is around 35% of that during spring tide for both cycles. Concerning the second cross-section (CP), located in the intersection of the Guadalquivir River and the tributary, Brazo de la Torre, during the neap tide, the volume of water flowing during the flood cycle is about 28%, and during the ebb cycle, it is approximately 35% compared to the spring tide results in CP. Comparing both sections, during spring tide, the volume of water that passes through the second section (CP) is only 4% and 3% for flood and ebb cycles, respectively, compared to the volume that flows through the first section (TP). As for neap tide, the volume that passes through CP is about 3% and 4% of the TP for the flood and ebb cycle, respectively.

In summary, this study primarily focusses on the impacts of sea level rise on the Guadalquivir Estuary and Doñana Marshes' hydrodynamics, namely, on maximum water levels, velocity, tidal asymmetry, and tidal prism. However, it is important to acknowledge that climate change may induce a range of other significant physical processes that affect estuarine dynamics, and that were not considered in this study. For instance, changes in precipitation patterns can lead to increased freshwater discharge, which, in turn, may alter salinity gradients and influence sediment transport within the estuary. Additionally, increased sediment discharge can result in significant morphological changes, including shifts in channel formation and estuarine bed elevations. These processes may further alter

tidal dynamics, contributing to changes in water levels, current velocities, and sedimentation patterns. While this analysis specifically addresses the effects of sea level rise on local tidal hydrodynamics, it is crucial to consider these broader climate change impacts in future studies to fully understand the complex interplay of factors affecting estuarine systems.

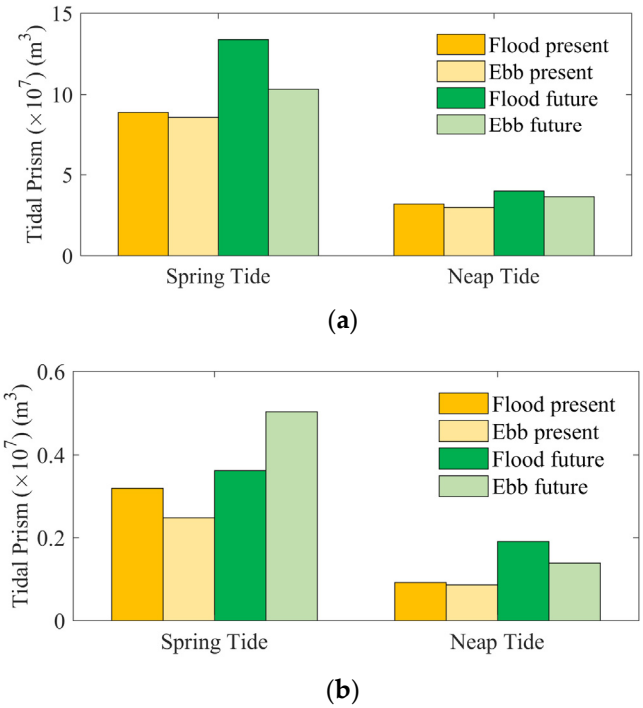

Figure 13. Flood and ebb tidal prism, during spring and neap tide conditions, for present and future conditions at cross-sections (**a**) TP and (**b**) CP.

5. Conclusions

This study deepens knowledge about the hydrodynamic characteristics of the Guadalquivir Estuary, both under present conditions and with a simulated removal of the existing dike infrastructure, aiming to understand how it would affect the Doñana Marshes and Guadalquivir Estuary dynamics under a climate change scenario. The results show that considering the present and future scenarios, the sea level rise together with the removal of the dike does affect the study area, flooding the entire Doñana Marshes during spring tide. This could lead to some negative effects since the environmental changes would be higher, leading to harder adaptation. However, this change could potentially alter the character of the marshes, transforming them into sinks for climate change gases. Currently, the marshes act as sources of CO_2 and CH_4 for the atmosphere. However, considering the effect of the dike removal and the sea level rise separately, no significant changes are predicted. The existing infrastructure continues to restrict most of the incoming water, even with a 0.84 m sea level rise.

While this study has provided valuable insights about the hydrodynamics of the Guadalquivir Estuary and Doñana Marshes, there is still a lack of scientific and technical information mostly in relation to water quality and the expected effects of salinisation on the wetland and the likely increase in aquatic alien species spread throughout the protected area due to water ballast by ship traffic.

Gathering more information on the Doñana Marshes and Guadalquivir Estuary, including an updated and more detailed digital elevation model from LiDAR, would certainly provide a more comprehensive understanding of the environment, especially regarding the impacts of extreme events related to expected effects of climate change. Additionally, the use of static bathymetry in this study is a limitation, as it does not account for potential sedimentation and long-term morphological changes due to sea level rise. Future research

should incorporate dynamic processes to better capture the complex interactions between hydrodynamics and morphology under changing sea levels. Nevertheless, the present study provides a useful first-order approximation of the system's response to sea level rise under the current conditions.

Likewise, it is crucial to improve our knowledge about climate change impacts for effective conservation and management strategies, especially in sensitive ecosystems like those of the Guadalquivir Estuary and Doñana Marshes, guiding the development of adaptive measures to mitigate potential negative impacts and preserve the ecological balance of the region.

Supplementary Materials: The following supporting information can be downloaded at https://www.mdpi.com/article/10.3390/jmse12081443/s1, Figure S1: Comparison of the time series of sea surface height between observed and predicted data at the (a) Bonanza, (b) Puntal, and (c) Caseta stations. The observed data are represented in blue (data), while the simulation results are illustrated in red.

Author Contributions: Conceptualisation, J.M.D. and A.P.; methodology, I.C., J.M.D. and A.P.; software, I.C., A.P. and M.D.; validation, I.C., M.D. and A.P.; formal analysis, I.C., A.P., M.D., A.L.-R., M.D.-M. and J.M.D.; investigation, I.C., A.P., M.D., A.L.-R., M.D.-M., R.D.-D., R.B. and J.M.D.; data curation, I.C., A.P., M.D., R.B. and R.D.-D.; writing—original draft preparation, I.C. and A.P.; writing—review and editing, I.C., A.P., M.D., A.L.-R., M.D.-M., R.D.-D., R.B. and J.M.D.; visualisation, I.C. and A.P.; supervision, J.M.D. and A.P.; funding acquisition, J.M.D. and M.D.-M. All authors have read and agreed to the published version of the manuscript.

Funding: Thanks are due to FCT/MCTES for the financial support to CESAM (UIDP/50017/2020 + UIDB/50017/2020 + LA/P/0094/2020). This work was partially founded by Junta de Andalucía–Consejería de Universidad, Investigación e Innovación–Proyecto ProyExcel_00375 (EPICOS) and the Multi-criteria analysis for Physical and bIotic Risk Assessment in EStuaries (PIRATES) Programme: Proyectos de I+D+i 2017. Programa Estatal de investigación, desarrollo e innovación orientada a los RETOS de la sociedad. M.Des was supported by the Xunta de Galicia through a postdoctoral grant ED481D-2024-018. R. Díaz-Delgado has benefited from "Salvador de Madariaga" mobility grant (PRX22/00726) funded by the Spanish Ministry of Science, Innovation and Universities (MICIU).

Institutional Review Board Statement: Not applicable.

Informed Consent Statement: Not applicable.

Data Availability Statement: Data available on request.

Acknowledgments: This work was performed in collaboration with the Doñana Biological Station and the EU Horizon 2020 project eLTER PLUS 'European long-term ecosystem, critical zone and socio-ecological systems research infrastructure PLUS' (grant agreement no. 871128) under task 8.1 'High resolution biodiversity data to assess environmental change'.

Conflicts of Interest: The authors declare no conflicts of interest.

References

1. Ramsar Convention. *An Introduction to the Ramsar Convention on Wetlands*, 7th ed.; previously The Ramsar Convention Manual; Ramsar Convention Secretariat: Gland, Switzerland, 2016.
2. Duarte, C.M.; Losada, I.J.; Hendriks, I.E.; Mazarrasa, I.; Marbà, N. The Role of Coastal Plant Communities for Climate Change Mitigation and Adaptation. *Nat. Clim. Chang.* **2013**, *3*, 961–968. [CrossRef]
3. Barbier, E.B.; Hacker, S.D.; Kennedy, C.; Koch, E.W.; Stier, A.C.; Silliman, B.R. The Value of Estuarine and Coastal Ecosystem Services. *Ecol. Monogr.* **2011**, *81*, 169–193. [CrossRef]
4. Howard, J.; Sutton-Grier, A.; Herr, D.; Kleypas, J.; Landis, E.; Mcleod, E.; Pidgeon, E.; Simpson, S. Clarifying the Role of Coastal and Marine Systems in Climate Mitigation. *Front. Ecol. Environ.* **2017**, *15*, 42–50. [CrossRef]
5. Ray, G.C. The Coastal Realm's Environmental Debt. *Aquat. Conserv.* **2006**, *16*, 1–4. [CrossRef]
6. Freeman, L.A.; Corbett, D.R.; Fitzgerald, A.M.; Lemley, D.A.; Quigg, A.; Steppe, C.N. Impacts of Urbanization and Development on Estuarine Ecosystems and Water Quality. *Estuaries Coast.* **2019**, *42*, 1821–1838.
7. Ekka, A.; Pande, S.; Jiang, Y.; Van Der Zaag, P. Anthropogenic Modifications and River Ecosystem Services: A Landscape Perspective. *Water* **2020**, *12*, 2706. [CrossRef]

8. Vu, H.L. Anthropogenic Influences on Ecosystem Processes in a Tropical Estuary: Feedback Connections and Environmental Management Targets A Case Study of Dong Ho Estuary, Kien Giang, Vietnam. Master's Thesis, The University of Queensland, St Lucia, QLD, Australia, 2018.
9. Llope, M. The Ecosystem Approach in the Gulf of Cadiz. A Perspective from the Southernmost European Atlantic Regional Sea. *ICES J. Mar. Sci.* **2017**, *74*, 382–390. [CrossRef]
10. Ruiz, J.; Polo, M.J.; Díez-Minguito, M.; Navarro, G.; Morris, E.P.; Huertas, E.; Caballero, I.; Contreras, E.; Losada, M.A. The Guadalquivir Estuary: A Hot Spot for Environmental and Human Conflicts. In *Coastal Research Library*; Springer: Berlin/Heidelberg, Germany, 2015; Volume 8, pp. 199–232.
11. Almaraz, P.; Green, A.J.; Aguilera, E.; Rendón, M.A.; Bustamante, J. Estimating Partial Observability and Nonlinear Climate Effects on Stochastic Community Dynamics of Migratory Waterfowl. *J. Anim. Ecol.* **2012**, *81*, 1113–1125. [CrossRef]
12. Washington State Department of Ecology Wetlands & Climate Change—Washington State Department of Ecology. Available online: https://ecology.wa.gov/Water-Shorelines/Wetlands/Tools-resources/Wetlands-climate-change (accessed on 13 October 2023).
13. Díez-Minguito, M.; Baquerizo, A.; Ortega-Sánchez, M.; Navarro, G.; Losada, M.A. Tide Transformation in the Guadalquivir Estuary (SW Spain) and Process-Based Zonation. *J. Geophys. Res. Oceans* **2012**, *117*, C03019. [CrossRef]
14. Spinosa, A.; Fuentes-Monjaraz, M.A.; El Serafy, G. Assessing the Use of Sentinel-2 Data for Spatio-Temporal Upscaling of Flux Tower Gross Primary Productivity Measurements. *Remote Sens.* **2023**, *15*, 562. [CrossRef]
15. IUCN; UNESCO World Heritage Centre. *Ramsar Secretariat Report on the Joint UNESCO/IUCN/Ramsar Reactive Monitoring Mission to Doñana National Park, Spain to 28 February 2020*; UNESCO World Heritage Centre: Gland, Switzerland, 2021.
16. Green, A.J.; Guardiola-Albert, C.; Bravo-Utrera, M.Á.; Bustamante, J.; Camacho, A.; Camacho, C.; Contreras-Arribas, E.; Espinar, J.L.; Gil-Gil, T.; Gomez-Mestre, I.; et al. Groundwater Abstraction Has Caused Extensive Ecological Damage to the Doñana World Heritage Site, Spain. *Wetlands* **2024**, *44*, 20. [CrossRef]
17. Díaz-Delgado, R. Cambio Global En Doñana: Seguimiento y Gestión. En: Los Humedales Costeros de La Península Ibérica. El Desafío Del Cambio Global. In *Los Humedales Costeros de la Península Ibérica*; Carles, S.I., Carles, I.M., Eds.; Tirant lo Blanch: Valencia, Spain, 2024; pp. 155–186, ISBN 9788411834858.
18. Sirviente, S.; Sánchez-Rodríguez, J.; Gomiz-Pascual, J.J.; Bolado-Penagos, M.; Sierra, A.; Ortega, T.; Álvarez, O.; Forja, J.; Bruno, M. A Numerical Simulation Study of the Hydrodynamic Effects Caused by Morphological Changes in the Guadalquivir River Estuary. *Sci. Total Environ.* **2023**, *902*, 166084. [CrossRef]
19. Muñoz-Lopez, P.; Nadal, I.; García-Lafuente, J.; Sammartino, S.; Bejarano, A. Numerical Modeling of Tidal Propagation and Frequency Responses in the Guadalquivir Estuary (SW, Iberian Peninsula). *Cont. Shelf Res.* **2024**, *279*, 105275. [CrossRef]
20. Gómez-Enri, J.; Aldarias, A.; Mulero-Martínez, R.; Vignudelli, S.; Bruno, M.; Mañanes, R.; Izquierdo, A.; Fernández-Barba, M. Satellite Radar Altimetry Supporting Coastal Hydrology: Case Studies of Guadalquivir River Estuary and Ebro River Delta (Spain). *IEEE J. Sel. Top. Appl. Earth Obs. Remote Sens.* **2024**, *17*, 3587–3599. [CrossRef]
21. Grimalt, J.O.; Ferrer, M.; Macpherson, E. The Mine Tailing Accident in Aznalcollar. *Sci. Total Environ.* **1999**, *242*, 3–11.
22. *Junta de Andalucía Guía Del y Su Entorno Espacio Natural de Doñana*, Seville, Spain, 2008; Volume 1a.
23. Gil, I.N.; de Mora, A.S.; Rodríguez, M.S.; Buzón, M.M. Donana y La Marisma. In *Programa de Educación Ambiental, Cuaderno de Campo*; Junta de Andalucía, Consejería de Medio Ambiente: Sevilla, Spain; pp. 1–48, ISBN 978-84-96776-87-6.
24. Siljeström, P.A.; Moreno, A.; Garcia, L.V.; Clemente, L.E. Doñana National Park (South-West Spain): Geomorphological Characterization through a Soil-Vegetation Study. *J. Arid. Environ.* **1994**, *26*, 315–323.
25. Rodríguez-Ramírez, A.; Yáñez-Camacho, C.M. Formation of Chenier Plain of the Doñana Marshland (SW Spain): Observations and Geomorphic Model. *Mar. Geol.* **2008**, *254*, 187–196. [CrossRef]
26. Barroso, P.; Acevedo, P.; Risalde, M.A.; García-Bocanegra, I.; Montoro, V.; Martínez-Padilla, A.B.; Torres, M.J.; Soriguer, R.C.; Vicente, J. Co-Exposure to Pathogens in Wild Ungulates from Doñana National Park, South Spain. *Res. Vet. Sci.* **2023**, *155*, 14–28. [CrossRef]
27. Gómez-Rodríguez, C.; Díaz-Paniagua, C.; Bustamante, J. Cartografía de Lagunas Temporales Del Parque Nacional de Doñana. 2011. Available online: https://www.researchgate.net/publication/236586598_Cartografia_de_lagunas_temporales_del_Parque_Nacional_de_Donana (accessed on 14 August 2024).
28. Donázar-Aramendía, I.; Sánchez-Moyano, J.E.; García-Asencio, I.; Miró, J.M.; Megina, C.; García-Gómez, J.C. Maintenance Dredging Impacts on a Highly Stressed Estuary (Guadalquivir Estuary): A BACI Approach through Oligohaline and Polyhaline Habitats. *Mar. Environ. Res.* **2018**, *140*, 455–467. [CrossRef]
29. Díez-Minguito, M.; Baquerizo, A.; Ortega-Sánchez, M.; Ruiz, I.; Losada, M.A. Tidal Wave Reflection from the Closure Dam in the Guadalquivir Estuary (SW Spain). *Coast. Eng. Proc.* **2012**, *1*, 58. [CrossRef]
30. Lee, J.; Biemond, B.; de Swart, H.; Dijkstra, H.A. Increasing Risks of Extreme Salt Intrusion Events across European Estuaries in a Warming Climate. *Commun. Earth Environ.* **2024**, *5*, 60. [CrossRef]
31. García-Lafuente, J.; Delgado, J.; Navarro, G.; Calero, C.; Díez-Minguito, M.; Ruiz, J.; Sánchez-Garrido, J.C. About the Tidal Oscillations of Temperature in a Tidally Driven Estuary: The Case of Guadalquivir Estuary, Southwest Spain. *Estuar. Coast. Shelf Sci.* **2012**, *111*, 60–66. [CrossRef]
32. Díez-Minguito, M.; Baquerizo, A.; De Swart, H.E.; Losada, M.A. Structure of the Turbidity Field in the Guadalquivir Estuary: Analysis of Observations and a Box Model Approach. *J. Geophys. Res. Oceans* **2014**, *119*, 7190–7204. [CrossRef]

33. Díaz-Delgado, R.; Aragonés, D.; Afán, I.; Bustamante, J. Long-Term Monitoring of the Flooding Regime and Hydroperiod of Doñana Marshes with Landsat Time Series (1974–2014). *Remote Sens.* **2016**, *8*, 775. [CrossRef]
34. Huertas, I.E.; Flecha, S.; Figuerola, J.; Costas, E.; Morris, E.P. Effect of Hydroperiod on CO2 Fluxes at the Air-Water Interface in the Mediterranean Coastal Wetlands of Doñana. *J. Geophys. Res. Biogeosci.* **2017**, *122*, 1615–1631. [CrossRef]
35. Huertas, I.E.; de la Paz, M.; Perez, F.F.; Navarro, G.; Flecha, S. Methane Emissions from the Salt Marshes of Doñana Wetlands: Spatio-Temporal Variability and Controlling Factors. *Front. Ecol. Evol.* **2019**, *7*, 32. [CrossRef]
36. García-Luque, E.; Forja, J.M.; Delvalls, T.A.; Gómez-Parra, A. The Behaviour of Heavy Metals from the Guadalquivir Estuary after the Aznalcóllar Mining Spill: Field and Laboratory Surveys. *Environ. Monit. Assess.* **2003**, *83*, 71–88. [CrossRef]
37. Omez-Parra, A.G.; Forja, J.M.; Delvalls, T.A.; Aenz, I.S.; Riba, I. Early Contamination by Heavy Metals of the Guadalquivir Estuary After the Aznalc Ollar Mining Spill (SW Spain). *Mar. Pollut. Bull.* **2000**, *40*, 1115–1123.
38. Diaz-Delgado, R.; Bustamante, J.; Aragonés, D. Hydroperiod of Doñana Marshes: Natural or Anthopic Origin of Inundation? *2006.* Available online: https://www.researchgate.net/publication/236586594_Hydroperiod_of_Donana_Marshes_Natural_or_Anthopic_Origin_of_Inundation_Regime (accessed on 14 August 2024).
39. Lesser, G.R.; Roelvink, J.A.; van Kester, J.A.T.M.; Stelling, G.S. Development and Validation of a Three-Dimensional Morphological Model. *Coast. Eng.* **2004**, *51*, 883–915. [CrossRef]
40. Wang, Z.B.; Winterwerp, J.C.; He, Q. Interaction between Suspended Sediment and Tidal Amplification in the Guadalquivir Estuary. *Ocean. Dyn.* **2014**, *64*, 1487–1498. [CrossRef]
41. Ibáñez Martínez, E. Validación de Modelos Digitales Del Terreno de Precisión a Partir de Datos Láser Escáner Aerotransportado; Aplicación a La Marisma Del Parque Nacional de Doñana. Ph.D. Thesis, Universitat Politècnica de Catalunya, Barcelona, Spain, 2008.
42. Navarro, G.; Gutiérrez, F.J.; Díez-Minguito, M.; Losada, M.A.; Ruiz, J. Temporal and Spatial Variability in the Guadalquivir Estuary: A Challenge for Real-Time Telemetry. *Ocean. Dyn.* **2011**, *61*, 753–765. [CrossRef]
43. Couto, I. Hydrodynamic Modeling in the Guadalquivir Estuary and Doñana National Park. Master's Thesis, University of Aveiro: Aveiro, Portugal, 2023.
44. Antunes, C.; Rocha, C.; Catita, C. Coastal Flood Assessment Due to Sea Level Rise and Extreme Storm Events: A Case Study of the Atlantic Coast of Portugal's Mainland. *Geosciences* **2019**, *9*, 239. [CrossRef]
45. Palmer, M.D.; Domingues, C.M.; A Slangen, A.B.; Boeira Dias, F. An Ensemble Approach to Quantify Global Mean Sea-Level Rise over the 20th Century from Tide Gauge Reconstructions. *Environ. Res. Lett.* **2021**, *16*, 044043. [CrossRef]
46. Pachauri, R.K.; Meyer, L.; Hallegatte France, S.; Bank, W.; Hegerl, G.; Brinkman, S.; van Kesteren, L.; Leprince-Ringuet, N.; van Boxmeer, F. IPCC Climate Change 2014: Synthesis Report. In *Contribution of Working Groups I, II and III to the Fifth Assessment Report of the Intergovernmental Panel on Climate Change*; Gian-Kasper Plattner: Geneva, Switzerland, 2014.
47. The Intergovernmental Panel on Climate Change AR6 Climate Change 2021: The Physical Science Basis—IPCC. Available online: https://www.ipcc.ch/report/sixth-assessment-report-working-group-i/ (accessed on 13 October 2023).
48. NASA. Sea Level Projection Tool. In *Sea Level Change Portal.*; 2023. Available online: https://sealevel.nasa.gov/ipcc-ar6-sea-level-projection-tool (accessed on 1 October 2023).
49. Latapy, A.; Héquette, A.; Nicolle, A.; Pouvreau, N. Influence of Shoreface Morphological Changes since the 19th Century on Nearshore Hydrodynamics and Shoreline Evolution in Wissant Bay (Northern France). *Mar. Geol.* **2020**, *422*, 106095. [CrossRef]
50. Pawlowicz, R.; Beardsley, B.; Lentz, S. Classical Tidal Harmonic Analysis Including Error Estimates in MATLAB Using T_TIDE. *Comput. Geosci.* **2002**, *28*, 929–937. [CrossRef]

Disclaimer/Publisher's Note: The statements, opinions and data contained in all publications are solely those of the individual author(s) and contributor(s) and not of MDPI and/or the editor(s). MDPI and/or the editor(s) disclaim responsibility for any injury to people or property resulting from any ideas, methods, instructions or products referred to in the content.